European Journal of Radiology 84 (2015) 811–815

Contents lists available at ScienceDirect

European Journal of Radiology

journal homepage: www.elsevier.com/locate/ejrad

Computer-aided assessment of hepatic contour abnormalities as an imaging biomarker for the prediction of hepatocellular carcinoma development in patients with chronic hepatitis C

Satoshi Goshima [a], Masayuki Kanematsu [a,*], Hiroshi Kondo [a], Haruo Watanabe [a], Yoshifumi Noda [a], Hiroshi Fujita [b], Kyongtae T. Bae [c]

[a] Department of Radiology, Gifu University Hospital, 1-1 Yanagido, 501-1194 Gifu, Japan
[b] Department of Intelligent Image Information Division of Regeneration and Advanced Medical Sciences, Graduate School of Medicine, Gifu University, Gifu, Japan
[c] Department of Radiology, University of Pittsburgh Medical Center, Pittsburgh, PA, USA

ARTICLE INFO

Article history:
Received 16 May 2014
Received in revised form 10 October 2014
Accepted 14 January 2015

Keywords:
MRI
Liver
Gadoxetic-acid
Cirrhosis
HCC

ABSTRACT

Purpose: To evaluate whether a hepatic fibrosis index (HFI), quantified on the basis of hepatic contour abnormality, is a risk factor for the development of hepatocellular carcinoma (HCC) in patients with chronic hepatitis C.

Materials and methods: Our institutional review board approved this retrospective study and written informed consent was waved. During a 14-month period, consecutive 98 patients with chronic hepatitis C who had no medical history of HCC treatment (56 men and 42 women; mean age, 70.7 years; range, 48–91 years) were included in this study. Gadoxetic acid-enhanced hepatocyte specific phase was used to detect and analyze hepatic contour abnormality. Hepatic contour abnormality was quantified and converted to HFI using in-house proto-type software. We compared HFI between patients with ($n = 54$) and without HCC ($n = 44$). Serum levels of albumin, total bilirubin, aspartate transferase, alanine transferase, percent prothrombin time, platelet count, alpha-fetoprotein, protein induced by vitamin K absence-II, and HFI were tested as possible risk factors for the development of HCC by determining the odds ratio with logistic regression analysis.

Results: HFIs were significantly higher in patients with HCC (0.58 ± 0.86) than those without (0.36 ± 0.11) ($P < 0.001$). Logistic analysis revealed that only HFI was a significant risk factor for HCC development with an odds ratio (95% confidence interval) of 26.4 (9.0–77.8) using a cutoff value of 0.395.

Conclusion: The hepatic fibrosis index, generated using a computer-aided assessment of hepatic contour abnormality, may be a useful imaging biomarker for the prediction of HCC development in patients with chronic hepatitis C.

1. Introduction

Chronic hepatitis C is a leading cause of hepatic fibrosis and hepatocellular carcinoma (HCC), both of which serve as major indications for liver transplantation [1,2]. The presence of cirrhosis is highly associated with HCC development in patients with chronic hepatitis C [3,4]. Pathologically, cirrhosis is the end stage of a variety of chronic diffuse liver diseases resulting in numerous nodules and fibrosis [5]. Detection and grading of hepatic fibrosis currently requires a biopsy, which is invasive and may potentially expose patients to a risk of serious complications. Indeed, a study that examined complications associated with over 68,000 percutaneous liver biopsies found a morbidity rate of 3% and a mortality rate of 0.03% [6]. Therefore, noninvasive methods, including ultrasonography [7] and MR elastography techniques [8,9], have been proposed and tested as a means to detect liver cirrhosis. Ultrasonographic features of liver surface nodularity are recognized as reliable predictors of severe liver fibrosis in patients with chronic hepatitis [10,11]. We previously reported a non-invasive computer-aided image analysis of hepatic contours that accurately detected hepatic fibrosis at stages F3 and F4 [12]. Furthering our investigation in this field, we also developed and tested semi-automated computer-aided diagnosis software that was based on the hepatic contour morphological features from MR images to improve the prediction

* Corresponding author. Tel.: +81 58 230 6439; fax: +81 58 230 6440.
E-mail address: masa.gif@yahoo.co.jp (M. Kanematsu).

http://dx.doi.org/10.1016/j.ejrad.2015.01.009
0720-048X/

of HCC development in patients with chronic hepatitis C. Thus, the purpose of this study was to demonstrate the clinical significance of the hepatic fibrosis index (HFI), quantified on the basis of hepatic contour abnormality, for the development of HCC in patients with chronic hepatitis C.

2. Materials and methods

2.1. Patients

Our institutional review board approved this retrospective study and written informed consent was waved. Between February 2012 and February 2013, 422 consecutive patients suspected of having chronic liver disease or focal hepatic lesions clinically or from previously performed ultrasonography or computed tomography (CT), underwent gadoxetic acid enhanced MR imaging in our department. In 188 of the 422 patients, hepatitis C was diagnosed by virus antibody detection. Among the 188 patients with chronic hepatitis C, we retrospectively included 98 patients who had no medical history of HCC treatment (56 men and 42 women; age range, 48–91 years; mean, 70.7 years). Among them, HCCs were identified in 54 patients (31 men and 23 women; age range, 48–91 years; mean, 71.6 years) by definitive surgery ($n = 15$), tumor biopsy ($n = 15$), and pathognomonic findings with combination CT hepatic arteriography and CT during arterial portography and lipiodolized CT after transcatheter arterial chemoembolization ($n = 24$). No HCC was found in the remaining 44 patients (25 men and 19 women; age range, 50–84 years; mean, 69.6 years;), in whom the absence of HCC was confirmed by follow-up gadoxetic acid-enhanced MR imaging performed in the following 3–6 months.

2.2. MR imaging techniques

MR imaging was performed using a 3-T MR system (Intera Achieva Quasar Dual; Philips Medical Systems, Netherlands) with a 6-channel torso array coil. The basic MR imaging protocol consisted of the following: breath-hold two-dimensional dual-echo axial T1-weighted fast field-echo (repetition time [TR]/echo time [TE], 292/2.3 ms at in-phase and 292/1.1 ms at opposed-phase); respiratory-triggered two-dimensional fat-suppressed axial T2-weighted turbo spin-echo (TR/TEeff 1600/80 ms); and breath-hold gadoxetic acid-enhanced hepatic arterial dominant-, portal venous-, and late dynamic-phase imaging with a fat-suppressed three-dimensional spoiled fast field-echo (TR/TE, 4.0/1.9 ms; field-of-view, 42×29 cm; 336×168 image matrix [512×512 reconstruction]; parallel imaging factor, 2.4; flip angle, 13°; slice thickness, 4.4-mm section thickness with 2.2-mm overlap; acquisition time, 90 slices per each phase during 20-s breath holding) imaging. Hepatocyte-phase images with the same three-dimensional spoiled fast field-echo sequence (except for a parallel imaging factor of 1 and acquisition of 90 slices during 22-s breath holding) were obtained 15–20 min (mean, 18.6 min) after an intravenous bolus injection of gadoxetic acid (Eovist or Primovist; Bayer Schering Pharma) at 0.025 mmol/kg body weight.

2.3. Quantitative image analysis

Quantitative analysis was conducted on a gadoxetic acid-enhanced hepatocyte-phase transaxial image using a prototype DICOM viewer. All measurements were performed by two radiologists in consensus (and with 5 and 13 years of post-training experience in interpreting body MR images, respectively) who had no knowledge of the clinical, hematological or radiological information regarding the patients. The hepatic contour abnormality was quantified on the right lobe at the hepatic hilar level and converted to HFI using in-house proto-type software. The algorithm consisted of following several steps.

i. Extraction of hepatic contour
   Gadoxetic acid-enhanced hepatocyte-phase transaxial image was converted to binary image. The hepatic contour was semi-automatically extracted using quarter pixel level plots on the arbitrary place of the right hepatic lobe at the hepatic hilar level (Fig. 1a).
ii. Calculation for the amount of characteristic
   The extracted hepatic contour line was represented on the X–Y coordinate to generate hepatic profile curves ($f_{(x)}$). An approximate curve ($D_{(x)}$) was then determined by a least-square approach with n-th degree polynomial equation that produced the highest R^2 value (Fig. 1b). Difference between the approximate curve of the hepatic profile ($D_{(x)}$) and ($f_{(x)}$) was calculated ($S_{(x)} = D_{(x)} - f_{(x)}$) (Fig. 1c). The 1 standard deviation (SD) of $S_{(x)}$ was expressed as HFI in this study.

Table 1
Patients characteristics.

	With HCC ($n = 54$)	Without HCC ($n = 44$)	P value
Patient age	71.5 (71.6, 48–91)	72.0 (69.6, 50–84)	0.34
Child-Pugh score (class)			
5–6 (A)	10	28	<0.001
7–9 (B)	35	12	<0.001
10–15 (C)	9	4	0.37
History of interferon therapy	36	27	0.67

2.4. Statistical analysis

Statistical analysis was performed using commercially available software (SPSS version 17.0, SPSS Inc., Chicago, IL). The relationship between HFI and Child-Pugh score was evaluated by calculating Pearson correlation coefficient. Patient age, gender, albumin, total bilirubin, aspartate transferase (AST) level, alanine transferase (ALT) level, percent prothrombin time, platelet count, alpha-fetoprotein (AFP), protein induced by vitamin K absence-II (PIVKA-II), and HFI were compared between patients with ($n = 54$) and without HCC ($n = 44$) using the Mann–Whitney U test, and were tested as a risk factor for the development of HCC as determined by the odds ratio with logistic regression analysis. Post hoc power analyses were performed in terms of the type II error and effect size using commercially available software (G*Power, version 3.1.2, University of Duesseldorf, Germany). P values of less than 0.05 were considered significant.

3. Results

Table 1d demonstrated background characteristics of the patients with and without HCC. No significant difference was found in patient age ($P = 0.34$). Significant differences were found in Child-Pugh score in lower classes ($P < 0.001$). There was no significant difference in the ratio of Child-Pugh class C ($P = 0.37$) and number of the patients with the history of interferon therapy ($P = 0.67$). HIF was significantly correlated with Child-Pugh score ($r = 0.85$, $P < 0.001$) (Fig. 2).

Quantitative values between two groups are summarized in Table 2. We found no significant difference in serum albumin ($P = 0.44$), total bilirubin ($P = 0.76$), AST ($P = 0.06$), ALT ($P = 0.58$), platelet count ($P = 0.27$), and percent prothrombin time ($P = 0.13$). However, the HFI ($P < 0.001$), alpha-fetoprotein ($P < 0.001$), and PIVKA-II ($P = 0.01$) were significantly higher in patients with HCC than those without HCC.

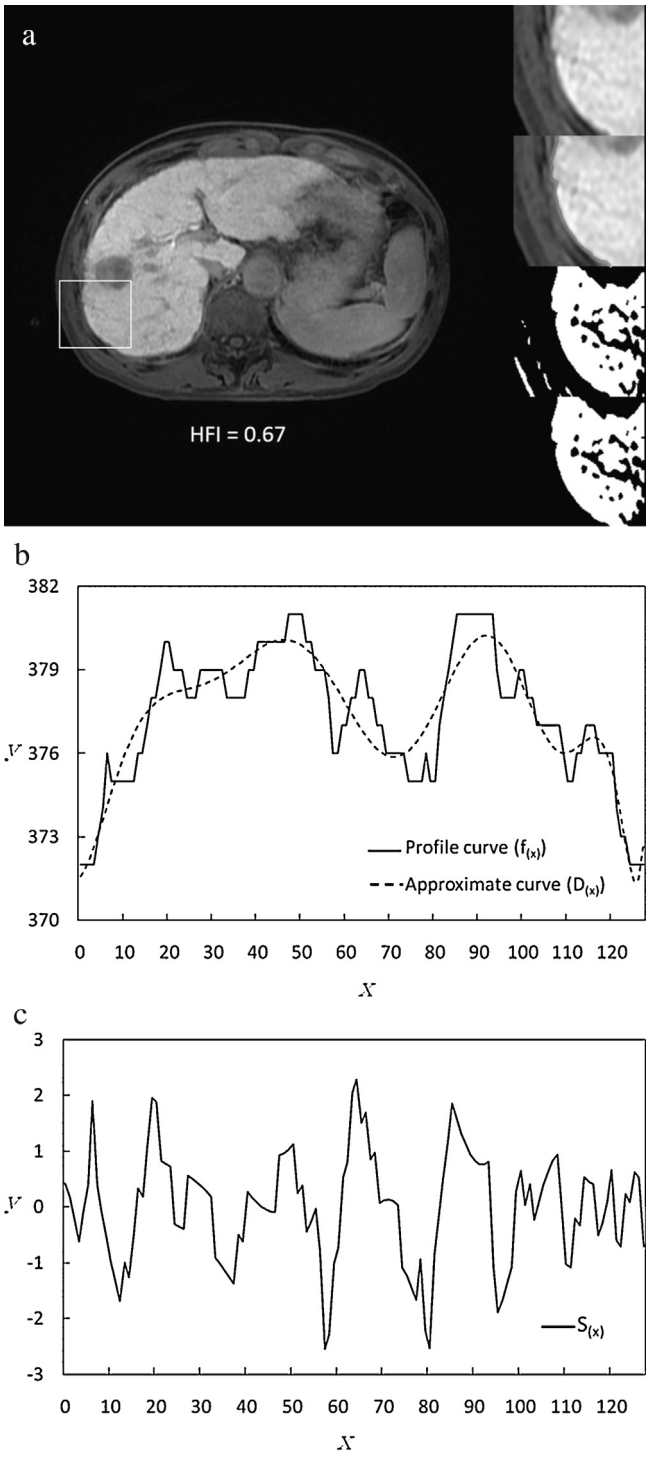

Fig. 1. 70-year-old man with HCC. (a) Gadoxetic acid-enhanced hepatocyte phase image obtained at hepatic hilar level was evaluated. Hepatic contour was semi-automatically profiled with 128 points of quarter pixel size at an arbitrary region using image thresholding. (b) Extracted hepatic contour was represented as hepatic profile curve ($f_{(x)}$). An approximate curve ($D_{(x)}$) was determined by a least-square approach with n-th degree polynomial equation which produced the highest R^2 value. (c) The difference between $D_{(x)}$ and $f_{(x)}$ was calculated ($S_{(x)} = D_{(x)} - f_{(x)}$) and then standard deviation of $S_{(x)}$ (SD) was expresses as HFI in this study.

Boxplots for HFI in the two patient groups are shown in Fig. 3. The HFI was significantly higher in patients with HCC (0.58 ± 0.86) than those without (0.36 ± 0.11) ($P < 0.001$). Logistic analysis revealed that only HFI was a significant risk factor for HCC, with an odds ratio (95% confidence interval) of 26.4 (9.0–77.8) using

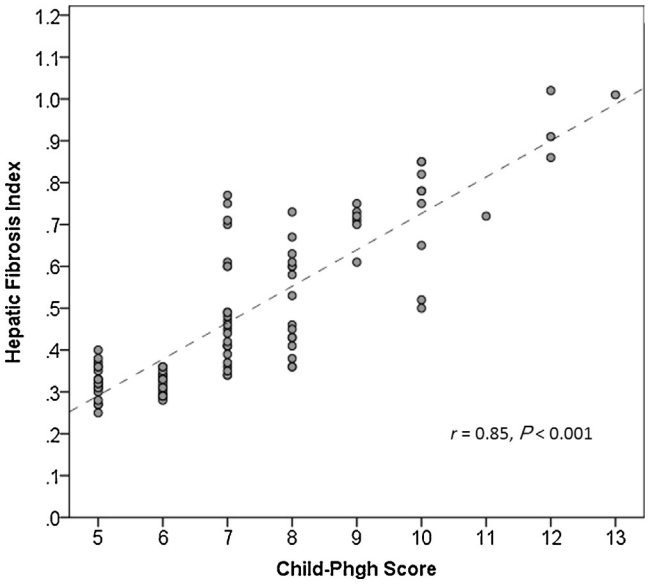

Fig. 2. Scatterplot showing the relationship between HFI and Child-Pugh score. There was a significant strong correlation between HFI and Child-Pugh score ($r = 0.85$, $P < 0.001$).

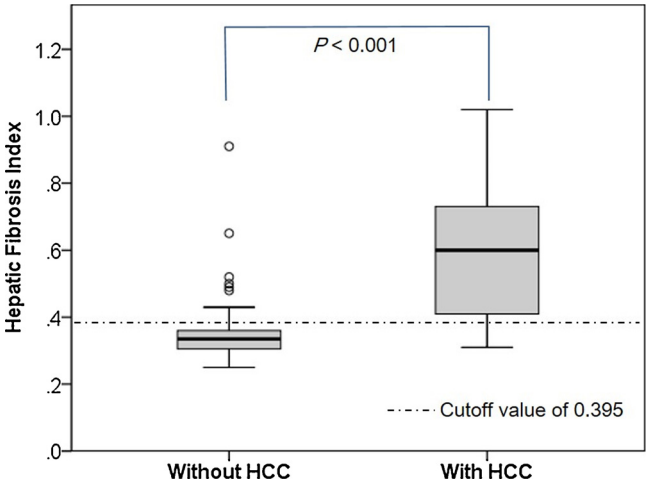

Fig. 3. Boxplots demonstrating HFI of the two groups. HFI was significantly higher in patients with HCC (0.58 ± 0.86) than without HCC (0.36 ± 0.11) with an odds ratio of 26.4 using a cutoff value of 0.395.

a cutoff value of 0.395. Post hoc power analysis showed that we had 79% power to detect a 5% difference between the patients with and without HCC.

4. Discussion

Previously reported risk factors for HCC development include advanced age, male gender, alcohol abuse, lower platelet count, high serum AFP level, low serum albumin level, high serum ALT level, and cirrhosis [13,14]. Among these risk factors, several studies have shown that the risk of HCC development in patients with chronic hepatitis C is higher in those with cirrhosis than in those with chronic hepatitis, although risk appears to vary geographically [15,16]. According to a large-scale study involving 490 untreated and 2400 interferon-treated patients with chronic hepatitis C, the annual incidence of HCC increased with the degree of liver fibrosis: untreated patients with stage F0 or F1 fibrosis had a 0.5% incidence that increased to 7.9% for patients with stage F4 fibrosis (cirrhosis); and interferon-treated patients with stage F0 or F1 fibrosis had a

Table 2
Comparison of patient age, hepatic fibrosis index, serological and tumor markers between the two groups.

	With HCC (n = 54)	Without HCC (n = 44)	P value
Hepatic fibrosis index	0.60 (0.58, 0.31–1.02)	0.34 (0.36, 0.25–0.91)	<0.001
Albumin (g/dL)	3.6 (3.5, 2.4–4.6)	3.7 (3.7, 1.6–5.0)	0.44
Total bilirubin (mg/dL)	1.0 (1.2, 0.4–3.1)	0.9 (1.2, 0.4–5.0)	0.76
AST (IU/L)	48.5 (60.5, 22–165)	41.0 (51.1, 9–195)	0.06
ALT (IU/L)	33.0 (46.2, 9–162)	39.5 (41.9, 10–182)	0.58
Platelet count (10^9/L)	9.4 (10.7, 3.2–35.2)	11.9 (12.0, 3.2–34.9)	0.27
Percent prothrombin time (%)	85.0 (82.7, 14–112)	89.5 (85.8, 34–120)	0.13
Alpha-fetoprotein (ng/mL)	23.8 (266.3, 2.1–6295)	6.3 (26.3, 2.1–382.8)	<0.001
PIVKA-II (mA U/mL)	34.0 (776.1, 6–28389)	19.0 (31.8, 7–158)	0.01

Note: Data are expressed as median.
The numbers in parentheses are mean and ranges.
PIVKA-II, protein induced by vitamin K absence-II.

0.08% incidence that increased to 4.2% for patients with stage F4 fibrosis [17].

Morphologic changes of the liver associated with cirrhosis include atrophy of the quadrate and the right lobe as well as hypertrophy of the left lateral segment and the caudate lobe [18]. Several reports [19–21] have proposed that a disproportionate decrease in the portal blood flow or differences in the concentrations of various hormones, hepatotrophic factors, and nutrients in the regional portal blood can contribute to the morphologic changes of the cirrhotic liver. At ultrasonographic scanning, liver surface nodularity reflects the presence of the regenerative nodules and fibrous septa that are the essential histologic findings for the diagnosis of cirrhosis [10,22]. Colli et al. [10,22] investigated the accuracy of various ultrasonographic signs to assess the degree of liver fibrosis, including surface nodularity and caudate lobe hypertrophy. Among these signs, the presence of hepatic surface nodularity revealed the highest diagnostic accuracy, with 95% specificity. Furthermore, a recent study using a computer-aided quantification and analysis reported that the hepatic surface nodularity on gadoxetic acid-enhanced MR images achieved a highly accurate diagnosis of hepatic fibrosis at stages F3 and F4 [12]. In our study, though we did not include the histopathological fibrosis information, HFI showed significant strong correlation with Child-Pugh score.

Recent studies have shown that gadoxetic acid-enhanced MR imaging readily detects early-stage HCCs [23,24]. Although qualitative, the detected imaging features were analyzed and applied to accurately diagnose HCCs. Our study presents the new perspective that some of the detected imaging features can be quantitatively analyzed and used not only for the diagnosis of HCCs, but also as biomarkers for HCC development. We demonstrated that HFI quantified on the basis of hepatic contour abnormality served as an independent, significant risk factor for HCC development as well as a potential biomarker for selecting patients at high risk for developing HCC, using routine gadoxetic acid-enhanced MR imaging. If indeed HFI identifies patients at high risk for HCC, then it could form the basis of a rationale surveillance for patients with chronic hepatitis C.

The quantification of HFI was performed on the gadoxetic acid-enhanced hepatocyte-phase transaxial images acquired using the three-dimensional spoiled fast field-echo sequence. The high contrast resolution with the fat-suppressed three-dimensional gradient-echo imaging of the liver facilitated the acquisition of thin-section images, increased the spatial resolution, and improved the accuracy in the extraction of hepatic contours. The gadoxetic acid contrast medium injected intravenously is gradually taken up by hepatocytes and eventually excreted via the biliary pathway. Peak liver signal intensity is noted 20 min after the injection, followed by a plateau-like enhancement of about 2 h duration [25]. Compared to MR imaging, contrast-enhanced CT images obtained during the portal venous phase also demonstrate excellent contrast of hepatic parenchyma [26,27]. We initially attempted to use CT images for the computer-aided hepatic contour analysis. However, in our implementation, we did not have success with CT images, largely because the contours of the liver were not sufficiently distinctive from the adjacent chest walls or hemidiaphragm on CT images.

There seems to be a strong relationship between the hepatic contour abnormality, the hepatic fibrosis stages [12] and HCC development. However, a variety of other hepatic pathologies may cause hepatic contour abnormality: Lipson et al. [28] report that hepatic contour abnormalities are often seen on CT or MR imaging, and that intrinsic disorders of the liver that might cause contour abnormalities consist of hepatic tumors, cirrhosis and confluent hepatic fibrosis, infarction and vascular occlusion, treatment change, and perihepatic diseases. Further study is necessary to assess the relationship between HFI and the other disease conditions that possibly cause hepatic contour abnormalities.

Our study has several limitations. First, this is a single-institution study using a single MR system. Likewise, this study had a relatively small sample size and study period. Although we demonstrated a very high odds ratio for the risk of HCC, a multi-center trial and longitudinal observation of a large population is required to confirm the generalizability of our finding. Second, we used a single slice image to generate the HFI in this study. Quantification of whole liver contour abnormality would be requested for the next trial. Third, we did not include other etiologies causing chronic hepatitis, such as type B hepatitis, alcohol abuse, or nonalcoholic steatohepatitis. Again, an additional study with a more diverse cohort is warranted to investigate the degree of other pathologies affecting hepatic morphological abnormalities.

In conclusion, we determined that the computer-generated, hepatic morphological index expressed as HFI was highly predictive for the development of HCC in patients with chronic hepatitis C. This index may serve as an important imaging biomarker for clinical management of these patients.

Conflicts of interest

We have no known conflicts of interest associated with this publication and there has been no significant financial support for this work that could have influenced its outcome.

Acknowledgment

The work was supported by Grant-in Aid for Scientific Research (KAKENHI) 24591752 of Japan.

References

[1] El-Serag HB, Mason AC. Rising incidence of hepatocellular carcinoma in the United States. New Engl J Med 1999;340:745–50.
[2] Poynard T, Yuen MF, Ratziu V, Lai CL. Viral hepatitis C. Lancet 2003;362: 2095–100.
[3] Tradati F, Colombo M, Mannucci PM, Rumi MG, De Fazio C, Gamba G, et al. A prospective multicenter study of hepatocellular carcinoma in Italian hemophiliacs with chronic hepatitis C. The Study Group of the Association of Italian Hemophilia Centers. Blood 1998;91:1173–7.
[4] Fattovich G, Giustina G, Degos F, Tremolada F, Diodati G, Almasio P, et al. Morbidity and mortality in compensated cirrhosis type C: a retrospective follow-up study of 384 patients. Gastroenterology 1997;112:463–72.
[5] Gebo KA, Herlong HF, Torbenson MS, Jenckes MW, Chander G, Ghanem KG, et al. Role of liver biopsy in management of chronic hepatitis C: a systematic review. Hepatology 2002;36:S161–72.
[6] Piccinino FSE, Pasquale G, Giusti G. Complications following percutaneous liver biopsy: a multicentre retrospective study on 68,276 biopsies. J Hepatol 1986;2:165–73.
[7] Friedrich-Rust M, Ong MF, Herrmann E, Dries V, Samaras P, Zeuzem S, et al. Real-time elastography for noninvasive assessment of liver fibrosis in chronic viral hepatitis. AJR Am J Roentgenol 2007;188:758–64.
[8] Huwart L, Sempoux C, Salameh N, Jamart J, Annet L, Sinkus R, et al. Liver fibrosis: noninvasive assessment with MR elastography versus aspartate aminotransferase-to-platelet ratio index. Radiology 2007;245:458–66.
[9] Rouviere O, Yin M, Dresner MA, Rossman PJ, Burgart LJ, Fidler JL, et al. MR elastography of the liver: preliminary results. Radiology 2006;240:440–8.
[10] Colli A, Fraquelli M, Andreoletti M, Marino B, Zuccoli E, Conte D. Severe liver fibrosis or cirrhosis: accuracy of US for detection – analysis of 300 cases. Radiology 2003;227:89–94.
[11] Vigano M, Visentin S, Aghemo A, Rumi MG, Ronchi G. US features of liver surface nodularity as a predictor of severe fibrosis in chronic hepatitis C. Radiology 2005;234:641, author reply.
[12] Goshima S, Kanematsu M, Kobayashi T, Furukawa T, Zhang X, Fujita H, et al. Staging hepatic fibrosis: computer-aided analysis of hepatic contours on gadolinium ethoxybenzyl diethylenetriaminepentaacetic acid-enhanced hepatocyte-phase magnetic resonance imaging. Hepatology 2012;55:328–9.
[13] Ikeda K, Saitoh S, Koida I, Arase Y, Tsubota A, Chayama K, et al. A multivariate analysis of risk factors for hepatocellular carcinogenesis: a prospective observation of 795 patients with viral and alcoholic cirrhosis. Hepatology 1993;18:47–53.
[14] Ikeda K, Saitoh S, Suzuki Y, Kobayashi M, Tsubota A, Koida I, et al. Disease progression and hepatocellular carcinogenesis in patients with chronic viral hepatitis: a prospective observation of 2215 patients. J Hepatol 1998;28:930–8.
[15] Chiaramonte M, Stroffolini T, Vian A, Stazi MA, Floreani A, Lorenzoni U, et al. Rate of incidence of hepatocellular carcinoma in patients with compensated viral cirrhosis. Cancer 1999;85:2132–7.
[16] Nishiguchi S, Shiomi S, Nakatani S, Takeda T, Fukuda K, Tamori A, et al. Prevention of hepatocellular carcinoma in patients with chronic active hepatitis C and cirrhosis. Lancet 2001;357:196–7.
[17] Yoshida H, Shiratori Y, Moriyama M, Arakawa Y, Ide T, Sata M, et al. Interferon therapy reduces the risk for hepatocellular carcinoma: national surveillance program of cirrhotic and noncirrhotic patients with chronic hepatitis C in Japan. IHIT Study Group. Inhibition of Hepatocarcinogenesis by Interferon Therapy. Ann Intern Med 1999;131:174–81.
[18] Awaya H, Mitchell DG, Kamishima T, Holland G, Ito K, Matsumoto T. Cirrhosis: modified caudate-right lobe ratio. Radiology 2002;224:769–74.
[19] Harbin WP, Robert NJ, Ferrucci Jr JT. Diagnosis of cirrhosis based on regional changes in hepatic morphology: a radiological and pathological analysis. Radiology 1980;135:273–83.
[20] Giorgio A, Amoroso P, Lettieri G, Fico P, de Stefano G, Finelli L, et al. Cirrhosis: value of caudate to right lobe ratio in diagnosis with US. Radiology 1986;161:443–5.
[21] Liu P, Li P, He W, Zhao LQ. Liver and spleen volume variations in patients with hepatic fibrosis. World J Gastroenterol 2009;15:3298–302.
[22] Schalm SW. The diagnosis of cirrhosis: clinical relevance and methodology. J Hepatol 1997;27:1118–9.
[23] Golfieri R, Renzulli M, Lucidi V, Corcioni B, Trevisani F, Bolondi L. Contribution of the hepatobiliary phase of Gd-EOB-DTPA-enhanced MRI to Dynamic MRI in the detection of hypovascular small ($\leq$2 cm) HCC in cirrhosis. Eur Radiol 2011;21:1233–42.
[24] Sano K, Ichikawa T, Motosugi U, Sou H, Muhi AM, Matsuda M, et al. Imaging study of early hepatocellular carcinoma: usefulness of gadoxetic acid-enhanced MR imaging. Radiology 2011;261:834–44.
[25] Hamm B, Staks T, Muhler A, Bollow M, Taupitz M, Frenzel T, et al. Phase I clinical evaluation of Gd-EOB-DTPA as a hepatobiliary MR contrast agent: safety, pharmacokinetics, and MR imaging. Radiology 1995;195: 785–92.
[26] Goshima S, Kanematsu M, Kondo H, Yokoyama R, Miyoshi T, Nishibori H, et al. MDCT of the liver and hypervascular hepatocellular carcinomas: optimizing scan delays for bolus-tracking techniques of hepatic arterial and portal venous phases. AJR Am J Roentgenol 2006;187:W25–32.
[27] Bae KT, Heiken JP, Brink JA. Aortic and hepatic peak enhancement at CT: effect of contrast medium injection rate – pharmacokinetic analysis and experimental porcine model. Radiology 1998;206:455–64.
[28] Lipson JA, Qayyum A, Avrin DE, Westphalen A, Yeh BM, Coakley FV. CT and MRI of hepatic contour abnormalities. AJR Am J Roentgenol 2005;184: 75–81.